Mechanism of sodium channel $Na_V1.9$ potentiation by G-protein signaling

Carlos G. Vanoye,[1] Jennifer D. Kunic,[1] George R. Ehring,[3] and Alfred L. George Jr.[1,2]

[1]Department of Medicine and [2]Department of Pharmacology, Vanderbilt University, Nashville, TN 37232
[3]Allergan, Inc., Irvine, CA 92623

Tetrodotoxin (TTX)-resistant voltage-gated Na (Na_V) channels have been implicated in nociception. In particular, $Na_V1.9$ contributes to expression of persistent Na current in small diameter, nociceptive sensory neurons in dorsal root ganglia and is required for inflammatory pain sensation. Using ND7/23 cells stably expressing human $Na_V1.9$, we elucidated the biophysical mechanisms responsible for potentiation of channel activity by G-protein signaling to better understand the response to inflammatory mediators. Heterologous $Na_V1.9$ expression evoked TTX-resistant Na current with peak activation at −40 mV with extensive overlap in voltage dependence of activation and inactivation. Inactivation kinetics were slow and incomplete, giving rise to large persistent Na currents. Single-channel recording demonstrated long openings and correspondingly high open probability (P_o) accounting for the large persistent current amplitude. Channels exposed to intracellular GTPγS, a proxy for G-protein signaling, exhibited twofold greater current density, slowing of inactivation, and a depolarizing shift in voltage dependence of inactivation but no change in activation voltage dependence. At the single-channel level, intracellular GTPγS had no effect on single-channel amplitude but caused an increased mean open time and greater P_o compared with recordings made in the absence of GTPγS. We conclude that G-protein activation potentiates human $Na_V1.9$ activity by increasing channel open probability and mean open time, causing the larger peak and persistent current, respectively. Our results advance our understanding about the mechanism of $Na_V1.9$ potentiation by G-protein signaling during inflammation and provide a cellular platform useful for the discovery of $Na_V1.9$ modulators with potential utility in treating inflammatory pain.

INTRODUCTION

Voltage-gated Na (Na_V) channels are critical for the initiation and propagation of action potentials in excitable tissues, including the brain and peripheral nerves. Two specific isoforms, $Na_V1.8$ and $Na_V1.9$ (also known as SNS and NaN, respectively), are tetrodotoxin (TTX)-resistant Na_V channels expressed in the peripheral nervous system (Dib-Hajj et al., 1998; Tate et al., 1998; Akopian et al., 1999; Persson et al., 2010). These channels are also found in the central nervous system (Jeong et al., 2000; Blum et al., 2002; O'Brien et al., 2008). Both $Na_V1.8$ and $Na_V1.9$ have been implicated in nociception, including neuronal pain signaling triggered by inflammation (Lai et al., 2004).

$Na_V1.8$ channels are expressed in retinal amacrine and ganglion cells (O'Brien et al., 2008), small and medium-sized dorsal root ganglion (DRG) neurons, and their nociceptive afferent fibers (Benn et al., 2001). In nociceptive fibers, $Na_V1.8$ channels are responsible for slowly inactivating Na currents that contribute to the depolarizing phase of action potentials in C-type small DRG neurons (Renganathan et al., 2001). $Na_V1.9$ channels are found in the hippocampus, cortex (Jeong et al., 2000; Blum et al., 2002), photoreceptors and Müller glia (O'Brien et al., 2008), small diameter, nociceptive sensory neurons in DRG (Fang et al., 2002), trigeminal ganglia, and in the intrinsic sensory neurons of the gut (Rugiero et al., 2003; Padilla et al., 2007). Compared with $Na_V1.8$ and TTX-sensitive neuronal channels, $Na_V1.9$ exhibits unique biophysical properties that include a hyperpolarized voltage-dependent activation, activation and inactivation curves that overlap near the resting membrane potential, slow activation and inactivation kinetics, and a very large persistent current (Cummins et al., 1999; Dib-Hajj et al., 2002; Coste et al., 2004). Persistent current generated by $Na_V1.9$ has been proposed to set thresholds for excitability of nociceptive sensory neurons by modulating both the resting potential and responses to subthreshold stimuli (Herzog et al., 2001; Priest et al., 2005; Ostman et al., 2008). A link between $Na_V1.9$-associated persistent current and pain sensation was demonstrated in neurons from $Na_V1.9$ knockout mice that lack persistent Na current and have greatly reduced inflammatory hyperalgesia (Priest et al., 2005; Amaya et al., 2006).

Correspondence to Alfred L. George Jr.: al.george@vanderbilt.edu

Abbreviations used in this paper: DRG, dorsal root ganglion; Na_V, voltage-gated Na; RT, room temperature; TTX, tetrodotoxin.

The Rockefeller University Press $30.00
J. Gen. Physiol. Vol. 141 No. 2 193–202
www.jgp.org/cgi/doi/10.1085/jgp.201210919

Inflammation caused by tissue damage results in pain, reflecting an increase in excitability of the primary afferent neurons innervating the area. Inflammatory agents such as bradykinin, ATP, histamine, prostaglandin E2, and norepinephrine potentiate $Na_V1.9$ current, increasing the excitability of DRG neurons, but these mediators fail to sensitize sensory neurons in $Na_V1.9$-null mice (Maingret et al., 2008a; Ritter et al., 2009). Studies using prostaglandin E2, protein kinase C, or G proteins also have demonstrated a link between inflammatory pathways and $Na_V1.9$-mediated nociceptor excitability (Baker et al., 2003; Baker, 2005). Together, these results indicate that $Na_V1.9$ contributes to the hyperexcitability of nociceptors observed during inflammatory pain. Inflammatory mediators that activate G-protein–dependent signal transduction increase the $Na_V1.9$ Na current (Rush and Waxman, 2004). Moreover, intracellular GTPγS (a hydrolysis-resistant GTP analogue) also potentiates persistent TTX-resistant Na current in wild-type and $Na_V1.8$-null mice sensory neurons (Baker et al., 2003) but does not increase persistent TTX-resistant Na current in small sensory neurons from $Na_V1.9$ knockout mice (Ostman et al., 2008). Discerning the mechanism for GTPγS potentiation of $Na_V1.9$ is important for understanding the encoding of painful sensations mediated by G-protein activation.

Heterologous expression of $Na_V1.9$ has proven difficult, and this has limited opportunities to elucidate functional properties of the channel and to implement small molecule screening assays to discover $Na_V1.9$ modulators. In this study, we used a highly efficient transposon system (Kahlig et al., 2010) to achieve stable expression of human $Na_V1.9$ in heterologous cells. This expression system allowed us to elucidate detailed biophysical properties of the channel, including the single-channel mechanism underlying potentiation by GTPγS. Our work further illustrates a cellular platform useful for the discovery of $Na_V1.9$ modulators that may have utility in treating chronic and inflammatory pain.

MATERIALS AND METHODS

Cell culture

All experiments were conducted using ND7/23 cells (Sigma-Aldrich) grown at 37°C with 5% CO_2 in Dulbecco's modified Eagle's medium (DMEM) supplemented with 10% fetal bovine serum (ATLANTA Biologicals), 2 mM L-glutamine, and 50 U/ml penicillin–50 µg/ml streptomycin. Unless otherwise stated, all tissue culture media was obtained from Life Technologies.

Plasmids and cell transfection

A full-length, human $Na_V1.9$ (GenBank accession no. NM_014139) cDNA including a C-terminal triple FLAG epitope (SRDYKDHDGDYKDHDIDYKDDDDKSR) was synthesized by DNA2.0 Inc. without codon optimization and cloned into a low copy number plasmid (pJ251). The FLAG epitope does not prevent plasma membrane trafficking of other neuronal Na_V channel proteins expressed heterologously or in vivo (Kearney et al., 2001; Kahlig et al., 2008). Stable expression of $Na_V1.9$-3xFLAG in ND7/23 cells was achieved using the *piggyBac* transposon system as previously described (Wilson et al., 2007; Kahlig et al., 2010) using a transposon vector containing a puromycin resistance gene (pB-$Na_V1.9$-3xFLAG-PuroR). ND7/23 cells were transfected with pCMV-hyPBase encoding a hyperactive version of the *piggyBac* transposase (Yusa et al., 2011) with pB-$Na_V1.9$-3xFLAG-PuroR using FUGENE-6 (Roche). Stable $Na_V1.9$-expressing cells were selected with 3 µg/ml puromycin (GIBCO/Invitrogen), and individual cell colonies were isolated using cloning discs and expanded.

$Na_V1.9$ protein expression

Cells were incubated at 37°C or 28°C with 5% CO_2 for ∼24 h before protein isolation. $Na_V1.9$ was detected using a monoclonal anti-FLAG antibody (Sigma-Aldrich). $Na_V1.9$-expressing cells (60-mm dishes) were washed twice with Dulbecco's PBS supplemented with $CaCl_2$ and $MgCl_2$ and then incubated with 1.5 mg/ml membrane-impermeant sulfo-NHS-biotin reagent (Thermo Fisher Scientific) for 1 h on ice. The cells were lysed with 500 µl RIPA buffer (150 mM NaCl, 50 mM Tris-Base, pH 7.5, 1% IGEPAL, 0.5% Na deoxycholate, and 0.1% SDS) supplemented with a Complete mini protease inhibitor tablet (Roche) and centrifuged at 14,000 *g* for 30 min at 4°C, and the supernatant fraction was collected and retained as the total lysate protein fraction. Protein lysates were quantified using the Bradford reagent (Bio-Rad Laboratories), and equal amounts of proteins were used in the immunoprecipitation experiments. The lysates were incubated with 50 µl ImmunoPure Immobilized Streptavidin beads (Thermo Fisher Scientific) overnight at 4°C. The samples were centrifuged for 10 s at 10,000 *g* and then washed three times with RIPA buffer at 4°C. The biotinylated proteins were eluted with 57 µl Laemmli sample buffer (Bio-Rad Laboratories) supplemented with 5% 2-mercaptanol (β-ME) for 30 min at room temperature (RT). Western blot analysis was performed by incubation for 1 h at RT with anti-FLAG diluted 1:15,000 for $Na_V1.9$ detection or anti-transferrin (GIBCO/Invitrogen) diluted 1:5,000 as a gel loading control. The secondary antibody (goat anti–mouse, same for both primary antibodies, diluted 1:10,000; Santa Cruz Biotechnology, Inc.) was horseradish peroxidase conjugated and incubated at RT for 1 h. Densitometry of protein bands was used to quantify protein levels (ImageJ software; National Institutes of Health). The $Na_V1.9$ band was normalized to the transferrin band to normalize for protein loading.

Electrophysiology

Cells were incubated at 28°C with 5% CO_2 for ∼24 h before their use in electrophysiology experiments. Cells were dissociated by trituration, resuspended in supplemented DMEM medium (without puromycin), plated on glass coverslips, and allowed to recover for ∼2 h before electrophysiological experiments. Cells were first maintained for 1 h at 37°C in 5% CO_2 and then at 28°C with 5% CO_2 until used in the experiments. For single-channel experiments, the glass coverslips were pretreated with CELL-TAK cell and tissue adhesive (Collaborative Biomedical Products).

Na currents were recorded at RT in the whole cell or excised, outside-out patch configuration of the patch-clamp technique (Hamill et al., 1981) using an Axopatch 200B series amplifier (Molecular Devices). Whole-cell currents were acquired at 20 kHz and filtered at 5 kHz. Pulse generation and data collection were performed with Clampex 9.2 (Molecular Devices). Bath solution contained (in mM) 145 NaCl, 4 KCl, 1.8 $CaCl_2$, 1 $MgCl_2$, and 10 HEPES (*N*-(2-hydroxyethyl)piperazine-*N*′-2-ethanosulphonic acid), pH 7.35, 310 mOsm/kg. 150 nM TTX was present in the bath to block endogenous Na currents. The

composition of the pipette solution was (in mM) 10 NaF, 110 CsF, 20 CsCl, 2 EGTA (ethyleneglycol-bis-(β-aminoethylether), and 10 HEPES, pH 7.35, 310 mOsm/kg. Osmolarity and pH values were adjusted with sucrose and NaOH, respectively. Whole-cell patch pipettes were pulled from thin-wall borosilicate glass, and single-channel patch pipettes were pulled from standard-wall borosilicate glass (Warner Instruments, LLC) with a multistage P-97 Flaming-Brown micropipette puller (Sutter Instrument) and fire-polished with a Micro Forge MF 830 (Narashige). Pipette resistance was ∼2 MΩ for whole-cell recording and 4–6 MΩ for outside-out patch recording. Single-channel recording pipettes were coated with Sylgard 184 (Dow Corning). 2% agar bridges containing bath solution served as reference electrodes.

Cells were allowed to equilibrate for 10 min in bath solution before obtaining seals. Peak currents were measured using 50-ms pulses to between −100 and 40 mV every 5 s from a holding potential of −120 mV. The peak current was normalized for cell capacitance and plotted against voltage to generate peak current density–voltage relationships. For recording of $Na_V1.9$ currents in low Na^+ bath solution ($[Na^+]_o$ = 20 mM), NaCl was replaced with equimolar *N*-methyl-D-glucamine-chloride (NMDG-Cl). The liquid junction potential generated upon reducing extracellular Na^+ was calculated using the Junction Potential Calculator in Clampex 9.2. The calculated junction potential was 4.5 mV. Whole-cell conductance was calculated from the peak current amplitude using the formula $G_{Na} = I_{Na}/(V - E_{rev})$, where E_{rev} is the estimated Na^+ reversal potential, and then normalized to the maximal conductance recorded between −80 and 20 mV. The normalized G-V curves were fit with the Boltzmann function, $G = 1/(1 + exp[(V - V_{1/2})/k])$, to determine the voltage for half-maximal channel activation ($V_{1/2}$) and slope factor (k). The voltage dependence of channel availability was assessed after a 300-ms prepulse to various potentials followed by 50-ms pulse to −40 mV, the voltage at which peak $Na_V1.9$ currents were measured. The normalized current was plotted against the voltage, and the steady-state channel availability curves were fit with Boltzmann functions ($I/Imax = 1/(1 + exp[(V - V_{1/2})/k])$ to determine the voltage for half-maximal channel inactivation ($V_{1/2}$) and slope factor (k). Recovery from fast inactivation was examined as fractional recovery against the recovery period and fitted to a five-parameter double exponential function, $I/I_{max} = A_f \times [1 - exp(-t/\tau_f)] + A_s \times [1 - exp(-t/\tau_s)] + C$, where τ_f and τ_s denote time constants (fast and slow components, respectively) and A_f and A_s represent the fast and slow fractional amplitudes. Single-channel behavior was examined during a −40-mV pulse from a holding potential of −120 mV in the presence of 150 nM external TTX. Single-channel currents were filtered at 2 kHz and acquired at 20 kHz. Each test pulse was followed by a 10-s recovery period at −120 mV. Linear leak and capacitive transients were subtracted using the mean of blank traces, and no corrections were made for missed events. The number of channels in each patch was determined as the maximum number of simultaneously open channels observed in all sweeps at a given voltage step. Only membrane patches without channel activity at the holding potential (−120 mV) or outward openings at the test potential (−40 mV) were analyzed, and this excluded contaminating currents from the other possible charge carriers present in the solutions (i.e., Ca^{2+}, F^-, and Cl^-).

Data analysis

Data were analyzed and plotted using a combination of Clampfit 9.2 (Molecular Devices), SigmaPlot 10 (Systat Software, Inc.) and Origin 7.0 (OriginLab). Statistical analyses were performed using SigmaStat 2.03 (Systat Software, Inc.), and statistical significance was determined using unpaired Student's *t* test. Data are represented as means ± standard error of the mean. The number of cells/patches used for each experimental condition is given in the figure legends.

RESULTS

Stable expression of human $Na_V1.9$

We generated a stable cell line expressing full-length, FLAG-tagged human $Na_V1.9$ cDNA ($Na_V1.9$-3xFLAG) in ND7/23 cells using a previously described transposon system (Wilson et al., 2007; Kahlig et al., 2010). We selected ND7/23 cells because of their chimeric derivation from rat DRG and mouse neuroblastoma cells and because our attempts to generate stably transfected HEK-293 and Chinese hamster ovary cells were unsatisfactory.

Initial electrophysiological analysis of $Na_V1.9$-expresing cells (performed in the presence of 150 nM TTX to block an endogenous TTX-sensitive Na_V channel) demonstrated small TTX-resistant currents (Fig. 1 A, top). Based on prior reports that low-temperature incubation of heterologous cells increased the functional expression of ion channels (e.g., CFTR and hERG; Denning et al., 1992; Zhou et al., 1999), we tested this strategy with $Na_V1.9$. Overnight incubation of $Na_V1.9$-ND7/23 cells at 28°C increased the current magnitude considerably (Fig. 1, A and B), whereas incubation of nontransfected ND7/23 cells at 28°C did not generate TTX-resistant currents. The $Na_V1.9$-dependent currents were markedly attenuated when the extracellular Na^+ concentration was reduced, consistent with an Na-selective channel (peak current: 145 mM external $[Na^+]$, 37.4 ± 13.2 pA/pF; 20 mM external $[Na^+]$, 6.5 ± 1.9 pA/pF; n = 5). Further, application of 30 µM TTX blocked peak current recorded at −40 mV by a mere 12.8 ± 2.9% (n = 4), consistent with a TTX-resistant channel.

Biochemical analysis of total and cell surface proteins isolated from $Na_V1.9$ stable cells cultured at 37°C and 28°C showed a prominent immunoreactive band (∼205 kD; Fig. 1 C) approximately the size predicted for native $Na_V1.9$. Previous analysis of $Na_V1.9$ protein from adult rat DRG neurons indicated that the channel is lightly glycosylated (Tyrrell et al., 2001), and this is consistent with our observation. Densitometry analysis of $Na_V1.9$ immunoblots (Fig. 1 C) demonstrated that total and cell surface $Na_V1.9$ protein expression were increased approximately twofold after overnight incubation of the cells at 28°C, but the molecular mass did not change (Fig. 1 D). The mean ratio of surface to total protein trended higher for cells incubated at 28°C (37°C = 0.8 ± 0.3; 28°C = 1.1 ± 0.3; n = 3), but the difference was not statistically significant.

Biophysical properties of human $Na_V1.9$

After establishing stable heterologous expression of $Na_V1.9$, we proceeded with determining more detailed functional properties of this unusual Na channel. As illustrated in Fig. 1 A, the kinetics of channel gating, especially inactivation, are markedly slow and have substantial voltage dependence. Furthermore, inactivation

at most test potentials is incomplete, producing large persistent Na currents. Activation of $Na_V1.9$ whole-cell current follows an exponential time course that is much slower than other mammalian Na_V channels (Fig. 2, A and B). For example, the time to peak activation for $Na_V1.9$ (9.4 ms at −30 mV; Fig. 2 B) is several fold slower than the TTX-sensitive $Na_V1.1$ (1.1 ms at −30 mV; Kahlig et al., 2008). Inactivation of $Na_V1.9$ is also slow and highly voltage sensitive (Fig. 2 C). At some test potentials (e.g., −80 mV), there was no measurable current decay, and the time course for the current recorded at this voltage was best fit with a linear equation. The time course of inactivation at other voltages was best fit with a single-exponential function from which we determined time constants. Inactivation is much slower than that reported for TTX-sensitive Na_V channels. For example, inactivation time constants at −40 mV for $Na_V1.1$ and $Na_V1.2$ are in the range of 1–2 ms (Lossin et al., 2002; Misra et al., 2008) as compared with ∼70 ms for $Na_V1.9$ (Fig. 2 D).

Steady-state inactivation and conductance-voltage (activation) curves have considerable overlap and intersect near −50 mV (Fig. 2 E). The intersection of these relationships at voltages near the resting potential of neurons predict a large window current, and this is consistent with previous explanations for the persistent Na current observed in DRG neurons (Herzog et al., 2001; Priest et al., 2005). The conductance-voltage relationship for $Na_V1.9$ (Fig. 2 E) exhibits a peculiar descent at potentials more positive than −30 mV. This phenomenon was previously observed in mouse DRG neurons (Cummins et al., 1999) but not in rat DRG or myenteric neurons (Tyrrell et al., 2001; Coste et al., 2004). We also measured recovery from inactivation after a 300-ms depolarization pulse to −40 mV. The recovery rate exhibited two exponential components with a predominant fast and a smaller slow component. Quantified biophysical parameters for the voltage dependence of activation, steady-state inactivation, and recovery from fast inactivation are provided in Table 1.

$Na_V1.9$ activation by GTPγS

Inflammatory mediators acting through G-protein–coupled receptors are known to potentiate $Na_V1.9$ channel activity and increase TTX-resistant persistent Na current in sensory neurons (Baker et al., 2003; Maingret et al., 2008b; Ostman et al., 2008; Ritter et al., 2009). These effects can be mimicked by intracellular application of GTPγS (a hydrolysis-resistant GTP analogue), and we tested whether this phenomenon could be replicated in $Na_V1.9$-expressing ND7/23 cells. Fig. 3 A illustrates the mean whole-cell currents recorded from $Na_V1.9$-expressing cells in the absence and presence of 200 µM of intracellular GTPγS. Application of intracellular GTPγS had a concentration-dependent effect on $Na_V1.9$ current density (Fig. 3, B and C). Addition of 20 µM GTPγS had no effect, whereas 63 µM increased the current density by 40% and 200 µM approximately doubled $Na_V1.9$ current density (Fig. 3, B and C). All subsequent experiments were performed with 200 µM GTPγS. The doubling of $Na_V1.9$ current density by GTPγS was evident 2 min after rupture of the membrane patch and intracellular dialysis with the pipette solution (Fig. 3 D). The increase in current density was accompanied by a depolarizing shift in the voltage dependence of inactivation without any effect on the

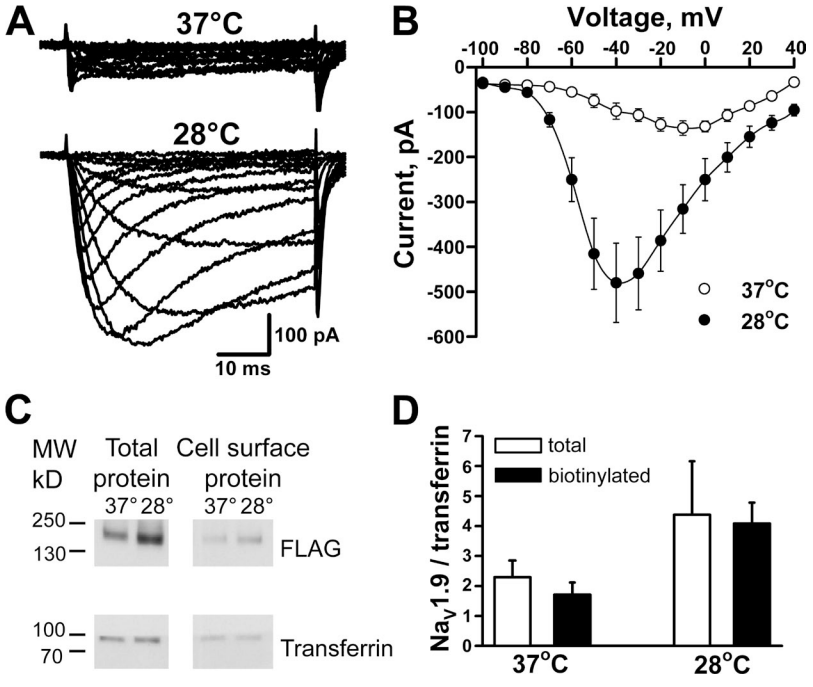

Figure 1. Incubation at 28°C increases $Na_V1.9$ cell surface expression and current magnitude. (A) Averaged whole-cell currents recorded from cells incubated at 37°C ($n = 8$) or 28°C ($n = 9$). (B) Current-voltage relationships measured from $Na_V1.9$-expressing cells at 37°C or 28°C. (C) Total and cell surface $Na_V1.9$ protein isolated from cells grown at 37°C or 28°C. (D) Densitometric analysis of total and cell surface $Na_V1.9$ bands obtained from three different protein isolations. Data are represented as means ± standard error of the mean.

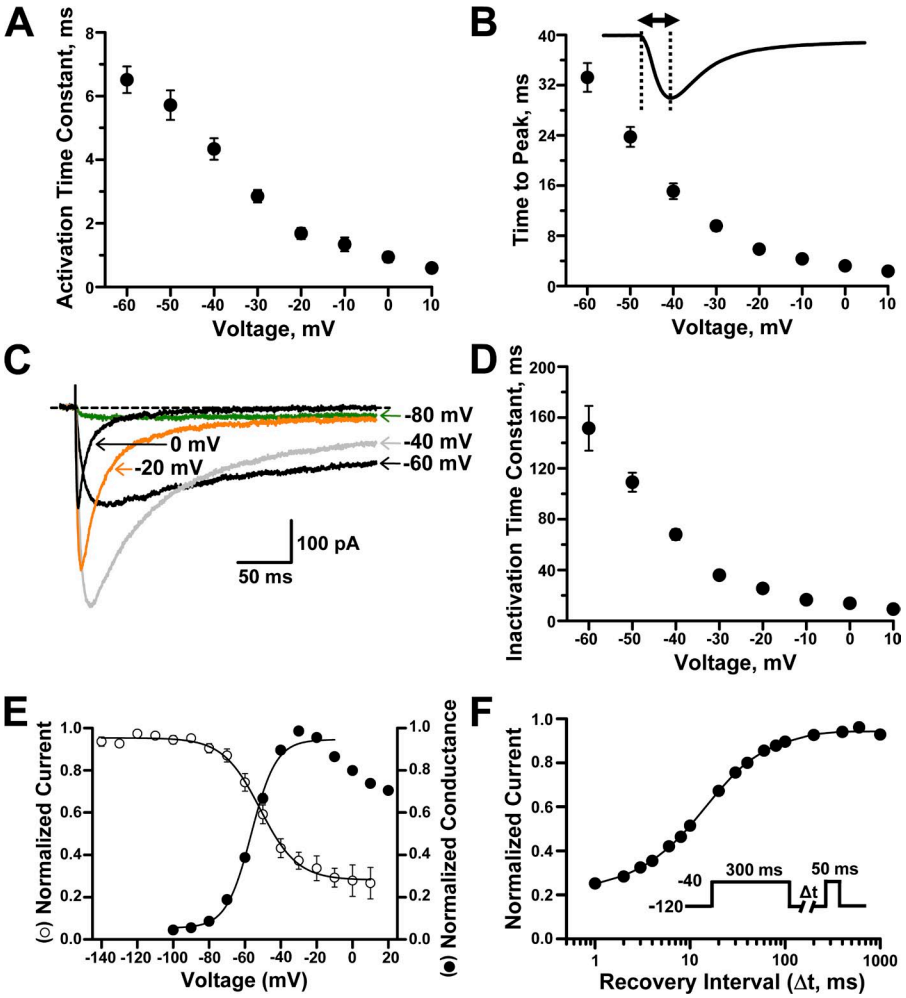

Figure 2. Biophysical properties of heterologously expressed human $Na_V1.9$. (A) Voltage dependence of activation time constants ($n = 14$–17). (B) Voltage dependence of time to peak current ($n = 18$). Solid line illustrates a representative inward current trace, dashed lines point to the beginning and peak of the current, and the double-headed arrow indicates the time to peak measurement period. (C) Mean whole-cell $Na_V1.9$ currents recorded during 300-ms pulses to −80, −60, −40, −20, and 0 mV ($n = 12$). Dashed line indicates the zero current level. (D) Voltage dependence of inactivation time constants ($n = 13$–17). (E) Superimposed steady-state channel availability (open circles) and conductance-voltage relationship (closed circles) for $Na_V1.9$ currents ($n =$ 7 and 16, respectively). Solid lines represent data fitted with Boltzmann functions. (F) Time course of recovery from fast inactivation (holding potential was −120 mV). Line represents data fitted with a two-exponential function ($n = 8$). Data are represented as means ± standard error of the mean.

voltage dependence of activation or the time course of recovery from inactivation (Fig. 3, E and F; and Table 1). Importantly, application of intracellular GTPγS did not evoke expression of TTX-resistant currents in nontransfected ND7/23 cells.

More detailed analyses revealed that intracellular GTPγS slightly decreased the slope factor for voltage dependence of activation and increased the time constant corresponding to the slow component of recovery from fast inactivation (Table 1). Whole-cell activation kinetics were not affected by intracellular GTPγS; both activation time constants (Fig. 4 A) and time to peak (Fig. 4 B) were similar to control values. However, GTPγS did affect inactivation kinetics at potentials

TABLE 1

Biophysical properties of $Na_V1.9$ in the absence (control) or presence of intracellular GTPγS

Condition	Peak current density (−40 mV)		Voltage dependence of activation			Steady-state inactivation			Recovery from inactivation		
	pA/pF	*n*	$V_{1/2}$	*k*	*n*	$V_{1/2}$	*k*	*n*	τ_1	τ_2	*n*
			mV			*mV*			*ms*	*ms*	
Control	−23.2 ± 3.4	16	−56.9 ± 0.6	6.7 ± 0.3	16	−52.1 ± 2.6	9.2 ± 0.7	7	13.6 ± 2.2 (52.3 ± 7.3%)	77.9 ± 11.5 (24.4 ± 6.9%)	8
GTPγS	−38.9 ± 5.1[a]	20	−54.3 ± 1.1	5.8 ± 0.3[b]	20	−43.6 ± 2.0[c]	10.4 ± 0.7	8	16.0 ± 1.0 (61.7 ± 3.9%)	466.9 ± 151.9[d] (18.0 ± 3.2%)	6

Steady-state inactivation was determined using a 300-ms prepulse to various potentials followed by a 50-ms pulse to −40 mV. Recovery from inactivation was determined after a 300-ms prepulse to −40 mV.

[a]P = 0.025 (GTPγS vs. control using Student's *t* test).

[b]P = 0.015 (GTPγS vs. control using Student's *t* test).

[c]P = 0.021 (GTPγS vs. control using Student's *t* test).

[d]P = 0.011 (GTPγS vs. control using Student's *t* test).

positive to −50 mV. Fig. 4 C shows whole-cell current inactivation of $Na_V1.9$ in the presence of intracellular GTPγS. Specifically, the inactivation time course determined between −40 mV and 10 mV exhibited a biexponential decay (Fig. 4 D) with voltage-dependent time constants and fractional amplitudes. At −40 mV, both the slow and fast components were equally proportioned, whereas at more positive potentials the fast component fraction predominated (∼65% at −20 mV and ∼80% at 10 mV, Fig. 4 E). These data indicated that GTPγS evoked changes in $Na_V1.9$ gating, but these findings from whole-cell recording experiments did not provide a clear explanation for increased current amplitude.

Single-channel mechanism of $Na_V1.9$ potentiation by GTPγS

To further elucidate biophysical mechanisms that explain GTPγS potentiation of $Na_V1.9$ current, we performed single-channel analysis on $Na_V1.9$-ND7/23 cells in the absence or presence of intracellular GTPγS. These experiments were performed in the presence of 150 nM external TTX to block endogenous Na_V channels. Fig. 5 illustrates representative single-channel traces recorded at −40 mV from excised outside-out membrane patches dialyzed with either control intracellular solution or with solution containing 200 μM GTPγS. Single-channel amplitudes were similar for both conditions (control, 0.69 ± 0.05 pA; +GTPγS, 0.72 ± 0.04 pA; Fig. 5 C). This observation excluded a fundamental change in ion permeation as the cause for increased whole-cell current amplitude evoked by GTPγS. In contrast, exposure of $Na_V1.9$ to intracellular GTPγS was associated with an ∼2.7-fold larger nP_o (control, 0.23 ± 0.07, $n = 4$; +GTPγS, 0.63 ± 0.05, $n = 4$; P = 0.004; Fig. 5 D) and a significantly greater mean open time deduced from open time histograms (Fig. 5 E). By dividing the nP_o value calculated for each outside-out patch by the maximum number of channels observed in the same patch, we calculated an ∼3.3-fold larger P_o for channels in the presence of GTPγS (P_o: control = 0.06 ± 0.01 [4.0 ± 1.3 channels/patch]; +GTPγS = 0.19 ± 0.02 [3.2 ± 0.2 channels/patch]). These findings indicated that changes in gating were primarily responsible for GTPγS potentiation of $Na_V1.9$ current.

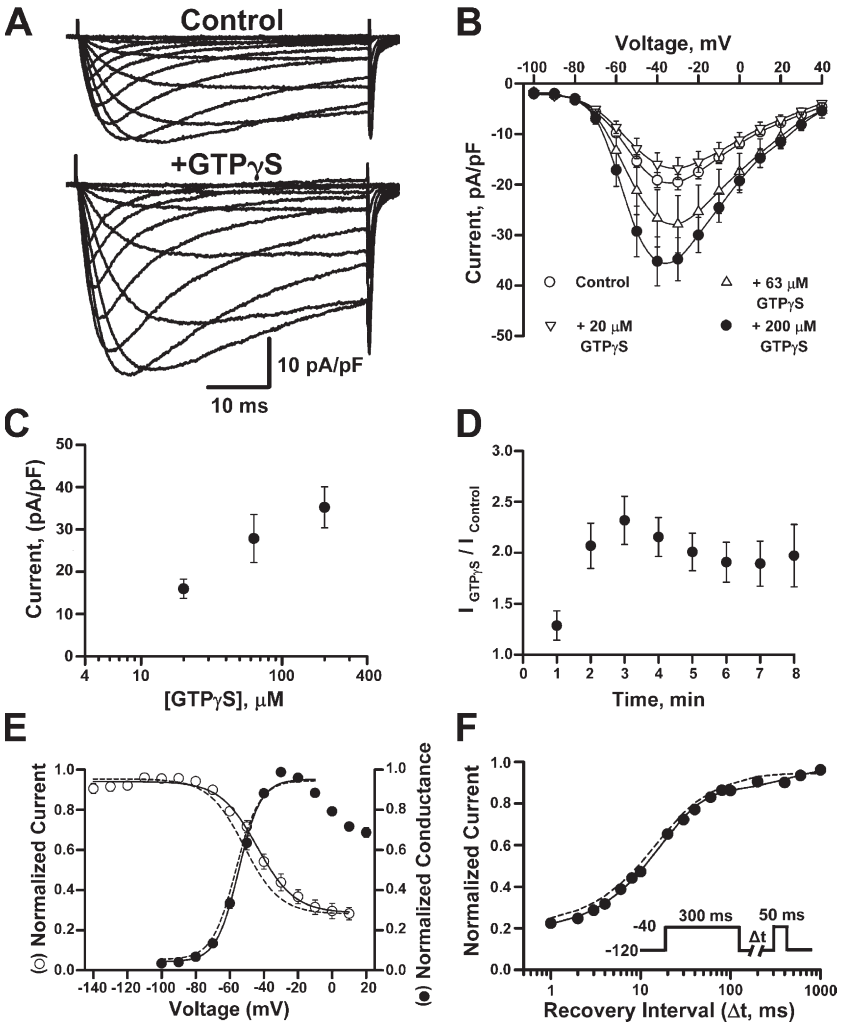

Figure 3. Intracellular GTPγS potentiates $Na_V1.9$ activity. (A) Averaged whole-cell currents recorded from $Na_V1.9$-expressing cells in the absence (control) or presence (+GTPγS) of 200 μM intracellular GTPγS. (B) Mean current-voltage relationships measured with control intracellular solution (n = 33) or with internal GTPγS at 20 μM (n = 9), 63 μM (n = 9), or 200 μM (n = 21). (C) Mean current density measured at −40 mV with control pipette or pipette plus GTPγS at 20 μM (n = 9), 63 μM (n = 9), or 200 μM (n = 21). (D) Whole-cell currents measured at −40 mV after rupture of membrane patch from cells dialyzed with 200 μM of intracellular GTPγS and normalized to the mean whole-cell current measured in cells dialyzed with control pipette solution (n = 8). (E) Superimposed steady-state channel availability (open circles) and conductance-voltage relationship (closed circles) recorded in the presence of intracellular GTPγS (n = 8 and 20, respectively). Dotted lines illustrate activation and inactivation curves determined in control solution (from Fig. 2 E). (F) Time course of recovery from fast inactivation (n = 8). Solid line represents data fitted with a two-exponential function. Dotted line depicts the recovery from inactivation recorded using control intracellular solution (from Fig. 2 F). Data are represented as means ± standard error of the mean.

DISCUSSION

In this study, we sought to determine the functional properties of recombinant human $Na_V1.9$ and the mechanism by which G-protein signaling increases $Na_V1.9$ activity. Because this Na_V channel has been implicated in nociception, our findings have implications for understanding the physiology of pain and could provide the basis for new analgesic strategies.

Heterologous functional expression of human $Na_V1.9$

Our experiments were enabled by successful and robust stable expression of human $Na_V1.9$ in heterologous cells. Previously, heterologous expression of $Na_V1.9$ has been difficult (Dib-Hajj et al., 2002), leading to speculation this is a not a voltage-gated channel, but rather a ligand-gated channel (Blum et al., 2002). However, the absence of TTX-resistant persistent Na current in mouse *Scn11A*-null neurons and its restoration by transfection of human $Na_V1.9$ in these cells (Ostman et al., 2008) eliminated doubt regarding the true nature of this protein.

Our success in achieving stable heterologous expression of $Na_V1.9$ can be attributed to three factors. First, we engineered $Na_V1.9$ stable cells using a highly efficient transposon system capable of integrating transgenes into multiple loci within a host cell genome (Kahlig et al., 2010). This approach may also bias integration events to regions of active chromatin increasing the likelihood of transgene expression (Wilson et al., 2007). Second, use of ND7/23 cells may provide intracellular factors expressed in neurons that are absent in other commonly used heterologous cells (e.g., HEK-293). For example, contactin has been demonstrated to bind to $Na_V1.9$ and increase surface expression and current density of $Na_V1.9$ channels in DRG neurons (Liu et al., 2001; Rush et al., 2005). Finally, we used low-temperature (28°C) incubation of cells to promote higher levels of functional $Na_V1.9$ expression. The efficacy of 28°C incubation to boost channel activity may reflect a certain degree of impaired $Na_V1.9$ trafficking in heterologous cells. However, our biochemical data did not demonstrate a clear change in the ratio of cell surface to total cellular protein consistent with

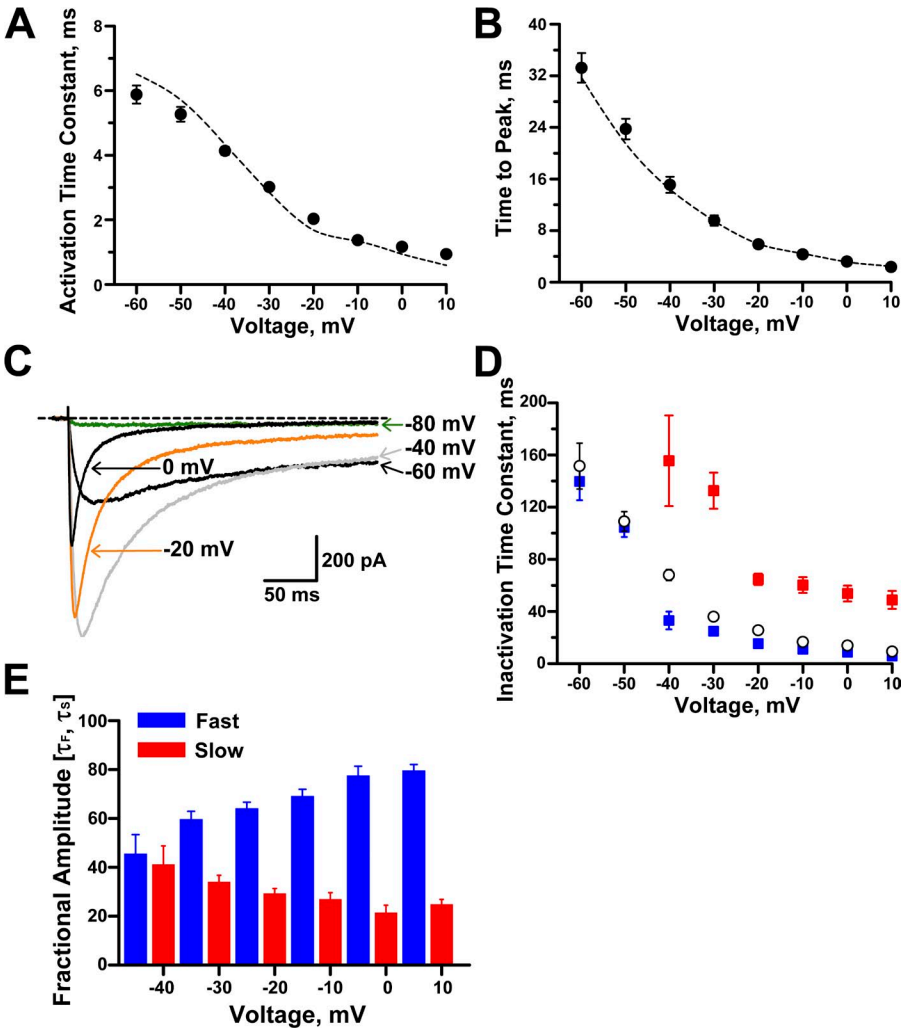

Figure 4. Effects of intracellular GTPγS on $Na_V1.9$ kinetics. (A) Time constants for activation in the presence of intracellular GTPγS (n = 13–14). (B) Time to peak current in the presence of intracellular GTPγS (n = 21). Dotted lines illustrate data for control solution (from Fig. 2). (C) Averaged whole-cell $Na_V1.9$ currents recorded during 300-ms pulses to −80, −60, −40, −20, and 0 mV. Dotted line indicates the zero current level (n = 10). (D) Inactivation time constants (fast, blue; slow, red) recorded in the presence of intracellular GTPγS (n = 8–14). Inactivation time constants for control pipette solution (open circles; n = 13–17) are also shown (from Fig. 2 D). (E) Fractional amplitudes for inactivation time constants determined in the presence of intracellular GTPγS for −40 to 10 mV (n = 8–14). Data are represented as means ± standard error of the mean.

redistribution of channels to the plasma membrane. Alternative explanations for the effects of low temperature include more efficient translation of $Na_V1.9$ or slower protein turnover. These various maneuvers appear to overcome the natural tendency for $Na_V1.9$ to express small Na currents, an intrinsic property of the channel which may protect cells from intracellular Na^+ overload or excessive membrane depolarization.

Biophysical properties of human $Na_V1.9$

Using stably expressing heterologous cells, we determined the biophysical properties of human $Na_V1.9$ using both whole-cell and single-channel recording strategies. Among the more characteristic features of $Na_V1.9$ is its unusually slow gating, especially inactivation. In single-channel recordings, long openings, and tendency for reopenings account for the sluggish nature of inactivation. This characteristic of $Na_V1.9$ inactivation stems in part from the large overlap between the voltage dependence of activation and inactivation with an expanded range of voltages in which channels are active but not subject to strong inactivation tendencies ("window" current). Furthermore, the voltage midpoint ($V_{1/2}$) for activation (−56 mV) is similar to that for inactivation (−52 mV). In contrast, fast-gating Na_V channels have inactivation $V_{1/2}$ values that are typically more negative than activation. The effect of this relationship is illustrated at −80 mV (Fig. 2 C), a voltage at which $Na_V1.9$ is activated but exhibits very little inactivation. Our findings are in agreement with previous experiments associating this channel with subthreshold Na current observed in sensory neurons. Some species-related differences in the reported voltage dependence of activation and inactivation for $Na_V1.9$ are evident when comparing our data with recordings from rats and mice (Cummins et al., 1999; Coste et al., 2004; Rush and Waxman, 2004), but the general trends are similar. However, the structural basis for the unusual gating behavior of $Na_V1.9$ is unclear.

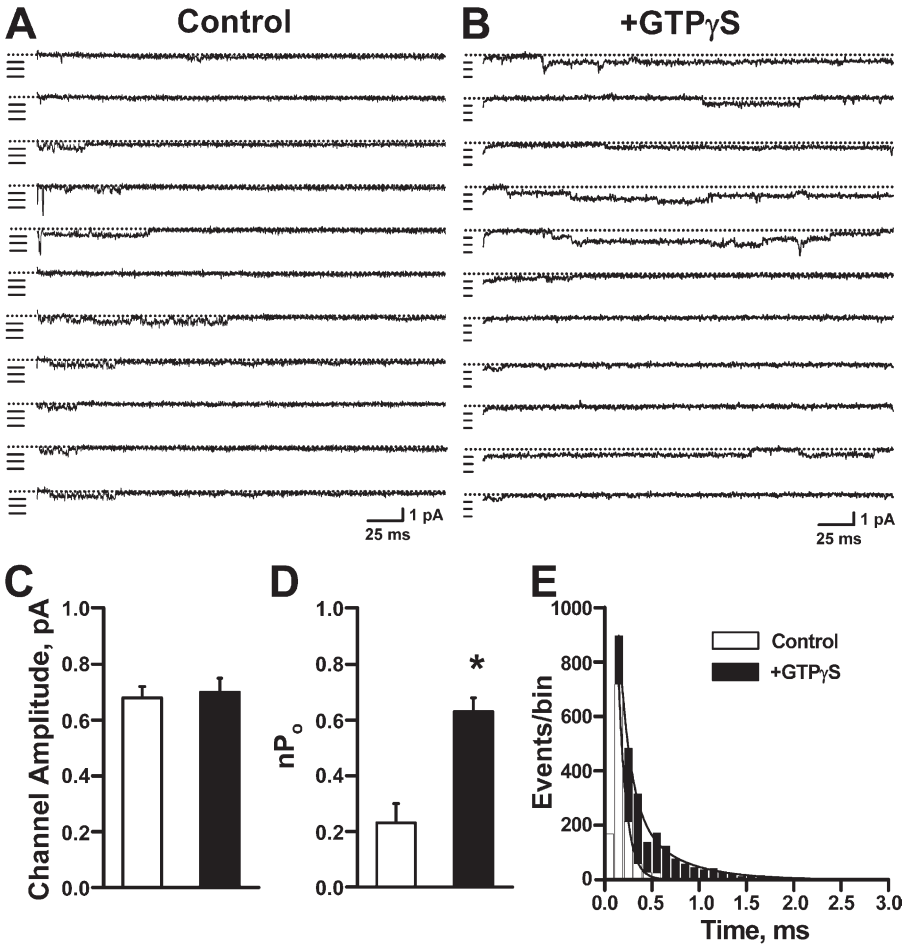

Figure 5. Effect of GTPγS on $Na_V1.9$ single-channel activity. Single $Na_V1.9$ channel openings were elicited by 300-ms pulses to −40 mV from a holding potential of −120 mV with 150 nM TTX present in the bath solution. (A) Single-channel traces from excised, outside-out patches dialyzed with control intracellular solution. Dotted lines indicate the zero current level, and individual single-channel amplitudes are marked by horizontal lines. The illustrated patch recordings contain at least six channels. (B) Single-channel traces from excised, outside-out patches dialyzed with pipette solution containing 200 µM GTPγS. The illustrated patch recordings contain at least four channels. (C) Single-channel amplitudes measured in the absence (control, $n = 4$) or presence (+GTPγS, $n = 4$) of 200 µM GTPγS. (D) Values for nP_o calculated from single-channel recordings from control and +GTPγS patches. Intracellular GTPγS increased nP_o ~2.5 (*, P = 0.004). (E) Open time histograms plotted for single-channel recordings performed in the absence or presence of GTPγS. The mean open times calculated for control solution were $\tau_1 = 0.09 \pm 0.01$ ms ($A_1 = 95.7 \pm 1.8\%$) and $\tau_2 = 0.47 \pm 0.07$ ms ($A_2 = 4.3 \pm 1.8\%$; $n = 4$). In the presence of GTPγS, mean open times were $\tau_1 = 0.24 \pm 0.05$ ms ($A_1 = 91.5 \pm 2.4\%$) and $\tau_2 = 1.55 \pm 0.35$ ms ($A_2 = 8.5 \pm 2.4\%$; $n = 4$). The differences in τ_1 and τ_2 values between control and +GTPγS were significant, P = 0.026 and P = 0.023, respectively. Data are represented as means ± standard error of the mean.

Mechanisms of GTPγS potentiation of human $Na_V1.9$

Previous studies have demonstrated that G-protein activation increases TTX-resistant, persistent Na current in sensory neurons and that this phenomenon requires $Na_V1.9$ (Baker et al., 2003; Rush and Waxman, 2004; Ostman et al., 2008). In this study, we demonstrated that heterologously expressed human $Na_V1.9$ can also be potentiated by intracellular GTPγS, a nonselective activator of G-protein signaling. We observed that exposure to GTPγS caused am approximate twofold greater current density accompanied by an ∼10-mV depolarizing shift in the voltage dependence of inactivation but without a change in activation voltage dependence. The unchanged voltage dependence of activation in combination with a more positive voltage dependence of inactivation yields a larger window current after GTPγS exposure. Additionally, GTPγS slowed inactivation by introducing a slower component readily discernable in a physiological voltage range. In contrast, study of murine $Na_V1.9$ demonstrated that $Na_V1.9$ potentiation by PGE_2 was accompanied by hyperpolarizing shifts in the voltage dependence of activation and inactivation but no effects on gating kinetics (Rush and Waxman, 2004). The different effects induced by G-protein activation on human or murine $Na_V1.9$ biophysical properties may be species or agonist specific. For example, GTPγS is a nonselective activator of G proteins, whereas PGE_2 signals through $G_{i/o}$ (Rush and Waxman, 2004). Our experiments were performed in the presence of intracellular fluoride, which may activate G proteins after binding to trace aluminum (Matzel et al., 1996). However, this did not prevent GTPγS modulation of $Na_V1.9$ channel activity.

To further elucidate the mechanism responsible for effects of intracellular GTPγS on $Na_V1.9$, we performed single-channel analysis. Our findings excluded a major change in permeation properties as the source for increased current density evoked by GTPγS. However, intracellular GTPγS did cause a significantly greater mean open time, which could account for the slower time course of inactivation and thus larger persistent current evoked by G-protein activation. We also examined whether channel open probability was affected. We determined that nP_o was ∼2.7 times greater in the presence than absence of intracellular GTPγS. Further analysis revealed that a greater P_o associated with GTPγS exposure closely approximates the fold increase in nP_o and whole-cell current density. Together, these results indicated that G-protein activation potentiates human $Na_V1.9$ by increasing channel open probability and lengthening mean open time, causing the larger peak and persistent current after exposure to inflammatory mediators.

In summary, we have developed a stable cell line expressing human $Na_V1.9$ and overcame previous challenges to investigating this channel in heterologous cells. We analyzed the biophysical properties of human $Na_V1.9$ and determined the mechanism by which GTPγS potentiates channel activity. Our results demonstrate a cellular platform that will be useful for the discovery of $Na_V1.9$ blockers or modulators and to understand how inflammatory agents regulate $Na_V1.9$ current. Furthermore, our findings may contribute to the development of new treatment strategies for chronic and inflammatory pain.

We would like to thank the Sanger Institute for providing the hyperactive *piggyBac* transposase plasmid.

This work was supported by a research grant from Allergan, Inc. and in part by National Institutes of Health grant NS032387 (to A.L. George Jr.). G.R. Ehring is a full-time employee of Allergan, Inc.

Christopher Miller served as editor.

Submitted: 23 October 2012
Accepted: 4 January 2013

REFERENCES

Akopian, A.N., V. Souslova, S. England, K. Okuse, N. Ogata, J. Ure, A. Smith, B.J. Kerr, S.B. McMahon, S. Boyce, et al. 1999. The tetrodotoxin-resistant sodium channel SNS has a specialized function in pain pathways. *Nat. Neurosci.* 2:541–548. http://dx.doi.org/10.1038/9195

Amaya, F., H. Wang, M. Costigan, A.J. Allchorne, J.P. Hatcher, J. Egerton, T. Stean, V. Morisset, D. Grose, M.J. Gunthorpe, et al. 2006. The voltage-gated sodium channel Na(v)1.9 is an effector of peripheral inflammatory pain hypersensitivity. *J. Neurosci.* 26:12852–12860. http://dx.doi.org/10.1523/JNEUROSCI.4015-06.2006

Baker, M.D. 2005. Protein kinase C mediates up-regulation of tetrodotoxin-resistant, persistent Na+ current in rat and mouse sensory neurones. *J. Physiol.* 567:851–867. http://dx.doi.org/10.1113/jphysiol.2005.089771

Baker, M.D., S.Y. Chandra, Y. Ding, S.G. Waxman, and J.N. Wood. 2003. GTP-induced tetrodotoxin-resistant Na+ current regulates excitability in mouse and rat small diameter sensory neurones. *J. Physiol.* 548:373–382. http://dx.doi.org/10.1113/jphysiol.2003.039131

Benn, S.C., M. Costigan, S. Tate, M. Fitzgerald, and C.J. Woolf. 2001. Developmental expression of the TTX-resistant voltage-gated sodium channels Nav1.8 (SNS) and Nav1.9 (SNS2) in primary sensory neurons. *J. Neurosci.* 21:6077–6085.

Blum, R., K.W. Kafitz, and A. Konnerth. 2002. Neurotrophin-evoked depolarization requires the sodium channel Na(V)1.9. *Nature.* 419:687–693. http://dx.doi.org/10.1038/nature01085

Coste, B., N. Osorio, F. Padilla, M. Crest, and P. Delmas. 2004. Gating and modulation of presumptive $Na_V1.9$ channels in enteric and spinal sensory neurons. *Mol. Cell. Neurosci.* 26:123–134. http://dx.doi.org/10.1016/j.mcn.2004.01.015

Cummins, T.R., S.D. Dib-Hajj, J.A. Black, A.N. Akopian, J.N. Wood, and S.G. Waxman. 1999. A novel persistent tetrodotoxin-resistant sodium current in SNS-null and wild-type small primary sensory neurons. *J. Neurosci.* 19:RC43.

Denning, G.M., M.P. Anderson, J.F. Amara, J. Marshall, A.E. Smith, and M.J. Welsh. 1992. Processing of mutant cystic fibrosis transmembrane conductance regulator is temperature-sensitive. *Nature.* 358:761–764. http://dx.doi.org/10.1038/358761a0

Dib-Hajj, S.D., L. Tyrrell, J.A. Black, and S.G. Waxman. 1998. NaN, a novel voltage-gated Na channel, is expressed preferentially in peripheral sensory neurons and down-regulated after axotomy.

Proc. Natl. Acad. Sci. USA. 95:8963–8968. http://dx.doi.org/10.1073/pnas.95.15.8963

Dib-Hajj, S., J.A. Black, T.R. Cummins, and S.G. Waxman. 2002. NaN/Nav1.9: a sodium channel with unique properties. *Trends Neurosci.* 25:253–259. http://dx.doi.org/10.1016/S0166-2236(02)02150-1

Fang, X., L. Djouhri, J.A. Black, S.D. Dib-Hajj, S.G. Waxman, and S.N. Lawson. 2002. The presence and role of the tetrodotoxin-resistant sodium channel Na(v)1.9 (NaN) in nociceptive primary afferent neurons. *J. Neurosci.* 22:7425–7433.

Hamill, O.P., A. Marty, E. Neher, B. Sakmann, and F.J. Sigworth. 1981. Improved patch-clamp techniques for high-resolution current recording from cells and cell-free membrane patches. *Pflugers Arch.* 391:85–100. http://dx.doi.org/10.1007/BF00656997

Herzog, R.I., T.R. Cummins, and S.G. Waxman. 2001. Persistent TTX-resistant Na+ current affects resting potential and response to depolarization in simulated spinal sensory neurons. *J. Neurophysiol.* 86:1351–1364.

Jeong, S.Y., J. Goto, H. Hashida, T. Suzuki, K. Ogata, N. Masuda, M. Hirai, K. Isahara, Y. Uchiyama, and I. Kanazawa. 2000. Identification of a novel human voltage-gated sodium channel alpha subunit gene, SCN12A. *Biochem. Biophys. Res. Commun.* 267:262–270. http://dx.doi.org/10.1006/bbrc.1999.1916

Kahlig, K.M., T.H. Rhodes, M. Pusch, T. Freilinger, J.M. Pereira-Monteiro, M.D. Ferrari, A.M. van den Maagdenberg, M. Dichgans, and A.L. George Jr. 2008. Divergent sodium channel defects in familial hemiplegic migraine. *Proc. Natl. Acad. Sci. USA.* 105:9799–9804. http://dx.doi.org/10.1073/pnas.0711717105

Kahlig, K.M., S.K. Saridey, A. Kaja, M.A. Daniels, A.L. George Jr., and M.H. Wilson. 2010. Multiplexed transposon-mediated stable gene transfer in human cells. *Proc. Natl. Acad. Sci. USA.* 107:1343–1348. http://dx.doi.org/10.1073/pnas.0910383107

Kearney, J.A., N.W. Plummer, M.R. Smith, J. Kapur, T.R. Cummins, S.G. Waxman, A.L. Goldin, and M.H. Meisler. 2001. A gain-of-function mutation in the sodium channel gene *Scn2a* results in seizures and behavioral abnormalities. *Neuroscience.* 102:307–317. http://dx.doi.org/10.1016/S0306-4522(00)00479-6

Lai, J., F. Porreca, J.C. Hunter, and M.S. Gold. 2004. Voltage-gated sodium channels and hyperalgesia. *Annu. Rev. Pharmacol. Toxicol.* 44:371–397. http://dx.doi.org/10.1146/annurev.pharmtox.44.101802.121627

Liu, C.J., S.D. Dib-Hajj, J.A. Black, J. Greenwood, Z. Lian, and S.G. Waxman. 2001. Direct interaction with contactin targets voltage-gated sodium channel Na(v)1.9/NaN to the cell membrane. *J. Biol. Chem.* 276:46553–46561. http://dx.doi.org/10.1074/jbc.M108699200

Lossin, C., D.W. Wang, T.H. Rhodes, C.G. Vanoye, and A.L. George Jr. 2002. Molecular basis of an inherited epilepsy. *Neuron.* 34:877–884. http://dx.doi.org/10.1016/S0896-6273(02)00714-6

Maingret, F., B. Coste, J. Hao, A. Giamarchi, D. Allen, M. Crest, D.W. Litchfield, J.P. Adelman, and P. Delmas. 2008a. Neurotransmitter modulation of small-conductance Ca2+-activated K+ channels by regulation of Ca2+ gating. *Neuron.* 59:439–449. http://dx.doi.org/10.1016/j.neuron.2008.05.026

Maingret, F., B. Coste, F. Padilla, N. Clerc, M. Crest, S.M. Korogod, and P. Delmas. 2008b. Inflammatory mediators increase Nav1.9 current and excitability in nociceptors through a coincident detection mechanism. *J. Gen. Physiol.* 131:211–225. http://dx.doi.org/10.1085/jgp.200709935

Matzel, L.D., R.F. Rogers, and A.C. Talk. 1996. Bidirectional regulation of neuronal potassium currents by the G-protein activator aluminum fluoride as a function of intracellular calcium concentration. *Neuroscience.* 74:1175–1185.

Misra, S.N., K.M. Kahlig, and A.L. George Jr. 2008. Impaired NaV1.2 function and reduced cell surface expression in benign familial neonatal-infantile seizures. *Epilepsia.* 49:1535–1545. http://dx.doi.org/10.1111/j.1528-1167.2008.01619.x

O'Brien, B.J., J.H. Caldwell, G.R. Ehring, K.M. Bumsted O'Brien, S. Luo, and S.R. Levinson. 2008. Tetrodotoxin-resistant voltage-gated sodium channels Na(v)1.8 and Na(v)1.9 are expressed in the retina. *J. Comp. Neurol.* 508:940–951. http://dx.doi.org/10.1002/cne.21701

Ostman, J.A., M.A. Nassar, J.N. Wood, and M.D. Baker. 2008. GTP up-regulated persistent Na+ current and enhanced nociceptor excitability require NaV1.9. *J. Physiol.* 586:1077–1087. http://dx.doi.org/10.1113/jphysiol.2007.147942

Padilla, F., M.L. Couble, B. Coste, F. Maingret, N. Clerc, M. Crest, A.M. Ritter, H. Magloire, and P. Delmas. 2007. Expression and localization of the Nav1.9 sodium channel in enteric neurons and in trigeminal sensory endings: implication for intestinal reflex function and orofacial pain. *Mol. Cell. Neurosci.* 35:138–152. http://dx.doi.org/10.1016/j.mcn.2007.02.008

Persson, A.K., J.A. Black, A. Gasser, X. Cheng, T.Z. Fischer, and S.G. Waxman. 2010. Sodium-calcium exchanger and multiple sodium channel isoforms in intra-epidermal nerve terminals. *Mol. Pain.* 6:84.

Priest, B.T., B.A. Murphy, J.A. Lindia, C. Diaz, C. Abbadie, A.M. Ritter, P. Liberator, L.M. Iyer, S.F. Kash, M.G. Kohler, et al. 2005. Contribution of the tetrodotoxin-resistant voltage-gated sodium channel NaV1.9 to sensory transmission and nociceptive behavior. *Proc. Natl. Acad. Sci. USA.* 102:9382–9387. http://dx.doi.org/10.1073/pnas.0501549102

Renganathan, M., T.R. Cummins, and S.G. Waxman. 2001. Contribution of Na(v)1.8 sodium channels to action potential electrogenesis in DRG neurons. *J. Neurophysiol.* 86:629–640.

Ritter, A.M., W.J. Martin, and K.S. Thorneloe. 2009. The voltage-gated sodium channel Nav1.9 is required for inflammation-based urinary bladder dysfunction. *Neurosci. Lett.* 452:28–32. http://dx.doi.org/10.1016/j.neulet.2008.12.051

Rugiero, F., M. Mistry, D. Sage, J.A. Black, S.G. Waxman, M. Crest, N. Clerc, P. Delmas, and M. Gola. 2003. Selective expression of a persistent tetrodotoxin-resistant Na+ current and NaV1.9 subunit in myenteric sensory neurons. *J. Neurosci.* 23:2715–2725.

Rush, A.M., and S.G. Waxman. 2004. PGE2 increases the tetrodotoxin-resistant Nav1.9 sodium current in mouse DRG neurons via G-proteins. *Brain Res.* 1023:264–271. http://dx.doi.org/10.1016/j.brainres.2004.07.042

Rush, A.M., M.J. Craner, T. Kageyama, S.D. Dib-Hajj, S.G. Waxman, and B. Ranscht. 2005. Contactin regulates the current density and axonal expression of tetrodotoxin-resistant but not tetrodotoxin-sensitive sodium channels in DRG neurons. *Eur. J. Neurosci.* 22:39–49. http://dx.doi.org/10.1111/j.1460-9568.2005.04186.x

Tate, S., S. Benn, C. Hick, D. Trezise, V. John, R.J. Mannion, M. Costigan, C. Plumpton, D. Grose, Z. Gladwell, et al. 1998. Two sodium channels contribute to the TTX-R sodium current in primary sensory neurons. *Nat. Neurosci.* 1:653–655. http://dx.doi.org/10.1038/3652

Tyrrell, L., M. Renganathan, S.D. Dib-Hajj, and S.G. Waxman. 2001. Glycosylation alters steady-state inactivation of sodium channel Nav1.9/NaN in dorsal root ganglion neurons and is developmentally regulated. *J. Neurosci.* 21:9629–9637.

Wilson, M.H., C.J. Coates, and A.L. George Jr. 2007. PiggyBac transposon-mediated gene transfer in human cells. *Mol. Ther.* 15:139–145. http://dx.doi.org/10.1038/sj.mt.6300028

Yusa, K., L. Zhou, M.A. Li, A. Bradley, and N.L. Craig. 2011. A hyperactive piggyBac transposase for mammalian applications. *Proc. Natl. Acad. Sci. USA.* 108:1531–1536. http://dx.doi.org/10.1073/pnas.1008322108

Zhou, Z., Q. Gong, and C.T. January. 1999. Correction of defective protein trafficking of a mutant HERG potassium channel in human long QT syndrome. Pharmacological and temperature effects. *J. Biol. Chem.* 274:31123–31126. http://dx.doi.org/10.1074/jbc.274.44.31123